

## High-spin states in $^{92}\text{Zr}^\dagger$

B. A. Brown,\* D. B. Fossan, P. M. S. Lesser, $^\ddagger$  and A. R. Poletti $^\S$   
*Department of Physics, State University of New York, Stony Brook, New York 11794*  
 (Received 27 April 1976)

High-spin states have been investigated with the  $^{88}\text{Sr}(^7\text{Li},p2n)^{92}\text{Zr}$  reaction by  $\gamma$ - $\gamma$  coincidence,  $\gamma$ -ray angular distribution, and pulsed beam- $\gamma$  timing measurements with Ge(Li) detectors. Decay schemes, level energies, and spin-parity information were obtained for  $^{92}\text{Zr}$  from the data. The high-spin states involving the  $(\pi 1g_{9/2})^2(\nu 2d_{5/2})^2$  configuration were identified, with the  $(12^+)$  member being at 4947 keV. Tentative identification of the members of the  $(\pi 1g_{9/2}\pi 2p_{1/2})(\nu 2d_{5/2})^2$  configuration has also been made. The observed experimental levels in  $^{92}\text{Zr}$  are compared with recent theoretical calculations.

NUCLEAR REACTIONS  $^{88}\text{Sr}(^7\text{Li},p2n)$   $E_{\text{Li}}=34$  MeV; measured  $\gamma$ - $\gamma$  coincidences,  $\gamma(E, \theta, t)$ ; deduced level scheme in  $^{92}\text{Zr}$ ,  $\gamma$  multiplicities,  $J^\pi$ . Natural target, Ge(Li) detectors.

### I. INTRODUCTION

The nuclei surrounding  $^{90}\text{Zr}$  are particularly simple to describe in the shell model because of the neutron-shell closure at  $N=50$ . In the first approximation the lowest  $0^+$ ,  $2^+$ , and  $4^+$  states in  $^{92}\text{Zr}$  are described by two neutrons in a  $(2d_{5/2})^2$  configuration outside  $N=50$  with the protons in the  $^{90}\text{Zr}$   $0^+$  ground-state configuration. A more complete description of  $^{92}\text{Zr}$  would include proton excitations to the well-known  $^{90}\text{Zr}$  excited states, $^1$  which involve the  $1g_{9/2}2p_{1/2}$  and  $(1g_{9/2})^2$  high-spin configurations, as well as neutron excitations to the  $3s_{1/2}$ ,  $2d_{3/2}$ ,  $1g_{7/2}$ , and  $1h_{11/2}$  orbitals. From the  $(\pi g_{9/2})^2(\nu d_{5/2})^2$  configuration, a maximum spin of  $12^+$  can be obtained. A knowledge of the high-spin members of this configuration in  $^{92}\text{Zr}$  is important for a complete comparison with theoretical calculations; presently, only members up to a spin of  $4^+$  are known. The negative-parity states involving the  $(\pi g_{9/2}\pi p_{1/2})(\nu d_{5/2})^2$  configuration with a maximum spin of  $9^-$  are likewise of interest.

In the present experiment,  $^{92}\text{Zr}$  was studied with the  $^{88}\text{Sr}(^7\text{Li},p2n)^{92}\text{Zr}$  fusion-evaporation reaction. This reaction favors the population of high-spin states aligned in low- $m$  substates whose dominant decay mode is via stretched  $\gamma$ -ray cascades down through the yrast levels $^2$  (states of lowest energy for a given spin). From the observed yrast  $\gamma$ -ray decay, positive parity levels up to an excitation energy of 5 MeV have been found with spins possibly as high as  $12^+$ . Several possible high-spin negative-parity states have also been located. No previous studies of these high-spin states have been carried out. A preliminary report of the present experiment has been made. $^3$

Previous experiments regarding  $^{92}\text{Zr}$  prior to 1972 are summarized in Nuclear Data Sheets. $^4$  More recent experiments are given in Refs. 5, 6, and 7. The previously established levels up to the  $3^-$  level at 2339 keV are shown in Fig. 1.

The present experiment was part of a series of investigations of high-spin states in the mass-90 region via fusion-evaporation reactions induced by  $^6\text{Li}$  and  $^7\text{Li}$  beams. $^{8,9}$  A complete discussion of the experimental techniques is given in Ref. 9 for the  $\text{Sr}+^7\text{Li}$  study of  $^{91}\text{Nb}$  and  $^{91}\text{Zr}$ . The same techniques, which are here briefly described in Sec. II, were utilized for the  $\text{Sr}+^7\text{Li}$  data presented in this paper. The experimental results for the  $^{92}\text{Zr}$  yrast decay are presented in Sec. III, and the energy levels are compared with recent theoretical calculations in Sec. IV.

### II. EXPERIMENTAL TECHNIQUE

Levels in  $^{92}\text{Zr}$  were populated via the fusion-evaporation reaction  $^{88}\text{Sr}(^7\text{Li},p2n)^{92}\text{Zr}$ . For most of the measurements, a 34-MeV  $^7\text{Li}(3^+)$  beam, obtained from the Stony Brook FN tandem Van de Graaff accelerator, was incident on a thick natural Sr metal target (82.6%  $^{88}\text{Sr}$ ) which stopped the beam. The beam energy was selected on the basis of  $\gamma$ -ray excitation measurements. Deexcitation  $\gamma$  rays were detected using both large volume Ge(Li) detectors for  $\gamma$  rays with  $100\text{ keV} < E_\gamma < 3\text{ MeV}$ , and a small planar intrinsic Ge detector for  $\gamma$  rays with  $20\text{ keV} < E_\gamma < 200\text{ keV}$ ; typical energy resolutions were 2.5–3 keV fullwidth at half maximum (FWHM) at 1332 keV, and 0.5 keV at 122 keV, respectively. Three types of experiments were carried out: (1)  $\gamma$ - $\gamma$  coincidence, (2)

$\gamma$ -ray angular distribution, and (3) pulsed-beam- $\gamma$  timing measurements.

Because of the complex nature of the  $\gamma$ -ray spectra from these reactions involving several residual nuclei,  $\gamma$ - $\gamma$  coincidence measurements with a Ge(Li)-Ge(Li) detector combination were required to identify the  $\gamma$ -ray cascades. To obtain information on the spins of the levels and the  $\gamma$ -ray multiplicities as well as the  $\gamma$ -ray intensities  $I_\gamma$ ,  $\gamma$ -ray angular distributions were measured in singles at seven angles between  $0^\circ$  and  $90^\circ$ . The photopeak areas were extracted and fitted to  $W(\theta) = I_\gamma(1 + A_2 P_2 + A_4 P_4)$ , where the  $P_k$  are the Legendre polynomials. Spin assignments were obtained from  $W(\theta)$ ,

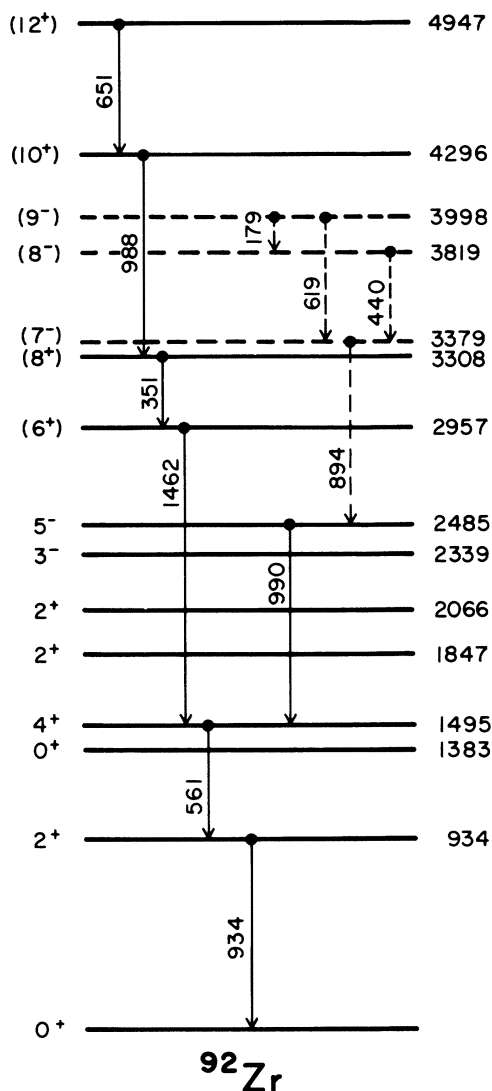


FIG. 1. The decay scheme for  $^{92}\text{Zr}$  high-spin levels from the present work. The non-yrast levels shown up to 2.4 MeV are from Ref. 4-7.

lifetime, and  $I_\gamma$  results. Finally, the observation of delayed  $\gamma$  rays with pulsed-beam timing allows the location of isomeric states and the study of their decay modes. Pulsed-beam measurements using the Ge(Li) and planar Ge detectors with overall time resolutions of  $\sim 8$  nsec FWHM were made with pulse repetition periods of 500 nsec and 1  $\mu$ sec.

### III. EXPERIMENTAL RESULTS

The singles  $\gamma$ -ray spectrum from the reactions induced by a 34-MeV  $^7\text{Li}$  beam on a thick natural Sr metal target is shown in Fig. 2.  $\gamma$  rays from the following nuclei were observed with the indicated relative yields that were estimated from all previously known transitions to the respective ground states:  $^{92}\text{Nb}$ (11),  $^{89}\text{Y}$ (7),  $^{91}\text{Nb}$ (6),  $^{92}\text{Zr}$ (3),  $^{90}\text{Zr}$ (2),  $^{90}\text{Y}$ (2),  $^{91}\text{Zr}$ (1), and  $^{88}\text{Y}$ (1). Several of these nuclei, in particular  $^{91}\text{Nb}$  and  $^{91}\text{Zr}$ , have been observed and studied independently via the  $\text{Sr} + ^6\text{Li}$  reaction.<sup>9</sup> The results for  $^{92}\text{Zr}$  are presented in detail below and the results for  $^{92}\text{Nb}$  will be presented elsewhere.<sup>10</sup>

Due to the complexity of the  $\gamma$  spectra, the  $\gamma$ - $\gamma$  coincidence measurements were essential for determining the  $\gamma$  rays which belong to  $^{92}\text{Zr}$ . All  $\gamma$  rays which have been placed into the  $^{92}\text{Zr}$  decay scheme were observed in coincidence with both the 561- and 934-keV  $\gamma$  rays from the well established 1495-keV  $\rightarrow$  934-keV  $\rightarrow$  ground-state cascade.<sup>4</sup> The  $\gamma$ - $\gamma$  coincidence spectra are shown in Fig. 3 and the coincident  $\gamma$  rays are listed in Table I.

From the delayed  $\gamma$  spectra, an upper limit of at least  $\tau \leq 5$  nsec was obtained for the mean lifetimes associated with all of the  $^{92}\text{Zr}$   $\gamma$  rays. For the highest energy  $\gamma$  ray observed in  $^{92}\text{Zr}$  at 1462 keV, this lifetime limit implies transition strengths of  $B(M2) \geq 0.07$  W.u. (Weisskopf units) and  $B(E3) \geq 50$  W.u. Since both of these are large compared with typical  $M2$  and  $E3$  strengths in the mass-90 region, all of the  $\gamma$  rays observed in  $^{92}\text{Zr}$  are most likely associated with  $E1$ ,  $M1$ , or  $E2$  transitions.

The most intense  $\gamma$  cascade feeding the 1495-keV level consists of four  $\gamma$  rays all in coincidence with each other; the order is established from the intensities obtained from the singles angular distribution measurements as 651-, 988-, 351-, and 1462 keV from the top and is confirmed by the coincidence yields (see Fig. 3). The angular distribution coefficients and the regular decrease in intensity with respect to increasing excitation energy (see Table II) indicates that these four  $\gamma$  rays, together with the 561- and 934-keV rays, form a sequence of six stretched-quadrupole  $J \rightarrow J-2$  transitions. The stretched-quadrupole assignments are strong for the 351-, 561-, and 934-keV

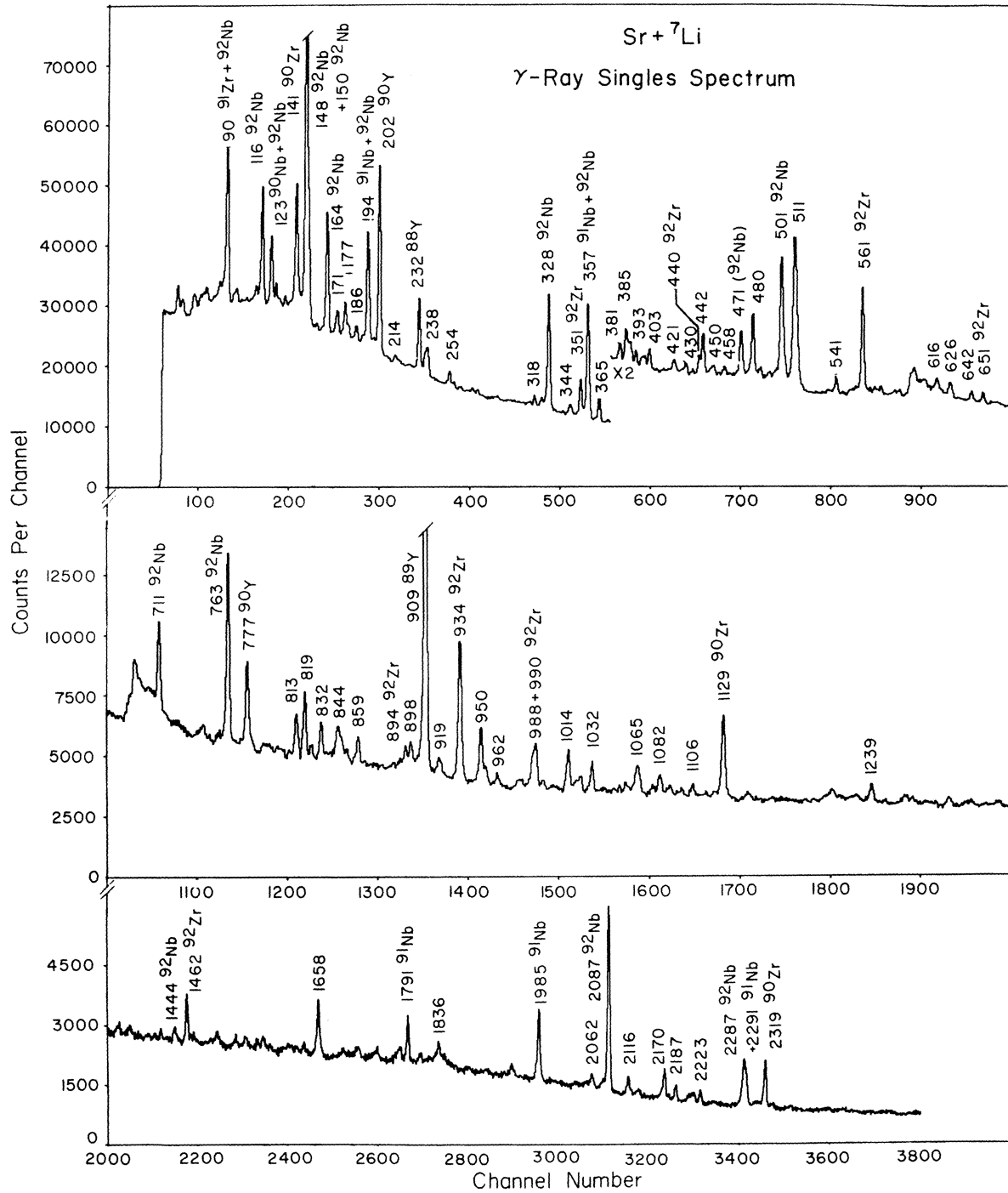


FIG. 2. The Ge(Li)  $\gamma$ -ray singles spectrum from the Sr(82.6%  $^{88}\text{Sr}$ ) +  $^7\text{Li}$  reaction. A thick metallic target and a 34-MeV energy were used. All strong  $\gamma$  rays which have been associated with  $^{92}\text{Zr}$  and  $^{92}\text{Nb}$  are labeled with the corresponding nucleus. A few of the  $\gamma$  rays from other nuclei are indicated, although the origins of most others not specifically labeled by a nucleus are known. At channel number 2000, the channel scale has been changed by a factor of 2.

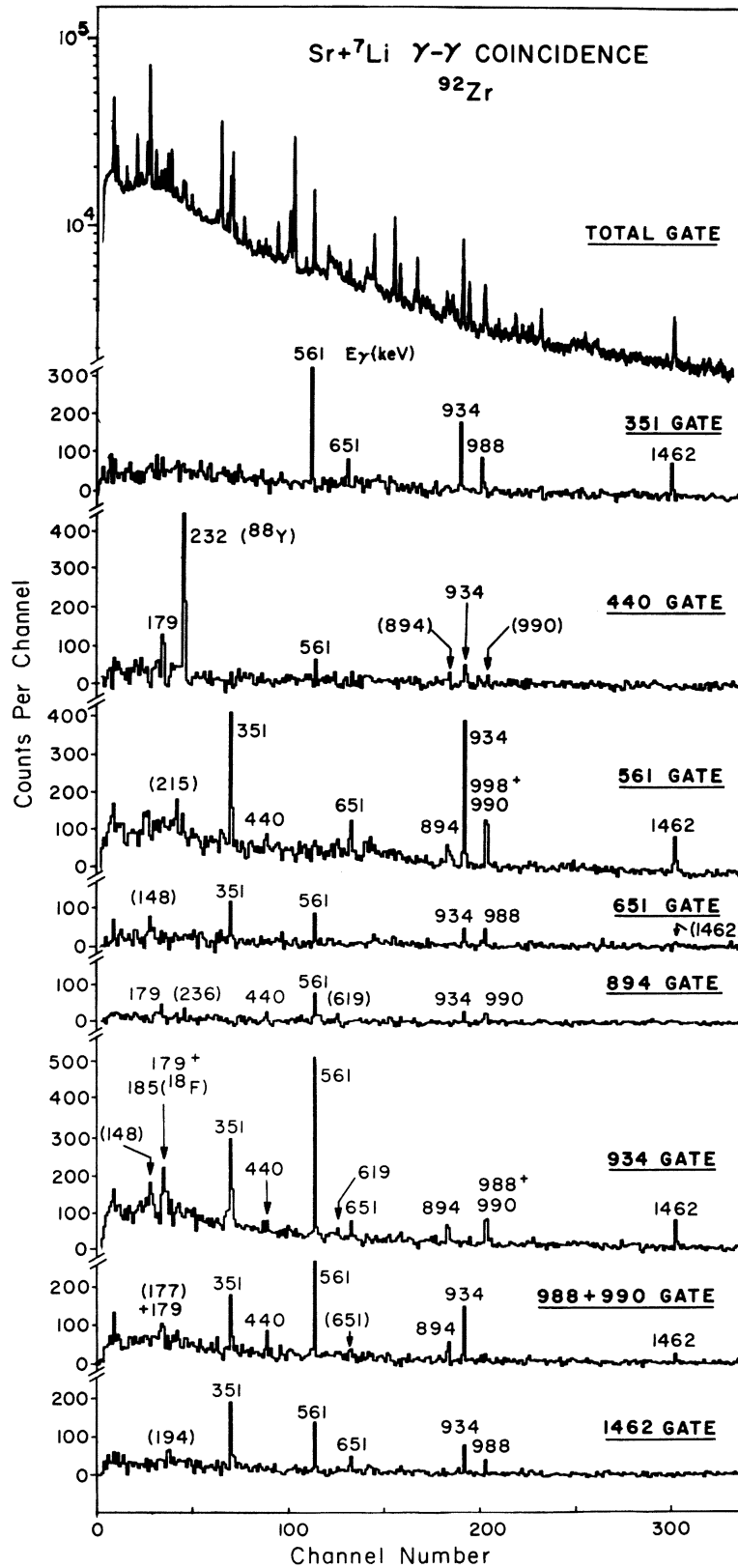


FIG. 3.  $\gamma$ - $\gamma$  coincidence spectra from  $^{92}\text{Zr}$   $\gamma$  rays. See Table I for a complete listing of the coincidence results.

TABLE I. Results of  $\gamma$ - $\gamma$  coincidence measurements for  $^{92}\text{Zr}$   $\gamma$  rays.

$\gamma$ ray in gate (keV)	Coincident $\gamma$ rays <sup>a</sup> (keV)
179	440, 561, 867, 894, 934, 990
351	561, 651, 934, 988, 1462
440	179, 232( $^{88}\text{Y}$ ), 561, (894), 934, (990)
561	(215), 351, (440), 651, 894, 934, 988, 990, 1462
651	(148), 351, 561, 934, 988, (1462)
894	179, (236), 440, 561, 619, 934, 990
934	(148), 179, 184( $^{18}\text{F}$ ), 351, 440, 561, 619, 651, 894, 988, 990, 1462
988 } 990 }	(177), 179, 351, 440, 561, (651), 894, 934, 1462
1462	(194), 351, 561, 651, 934, 988

<sup>a</sup> Coincident  $\gamma$  rays which are uncertain are put in brackets.

$\gamma$  rays due to the small uncertainty in the experimental  $A_2$  and  $A_4$  coefficients. However, the larger uncertainty in the angular distribution coefficients for the weaker 651-, 988-, and 1462-keV  $\gamma$  rays, especially for the  $A_4$  coefficient which is essential in establishing a definite  $L=2$  character, make the stretched-quadrupole assignment for these  $\gamma$  rays more tentative. Thus the following levels and spins are deduced (see Fig. 1): 934-keV  $2^+$ , 1495 keV  $4^+$ , 2957 keV ( $6^+$ ), 3308 keV ( $8^+$ ), 4296 keV ( $10^+$ ), and 4947 keV ( $12^+$ ).

An upper limit for the mean lifetime of  $\tau \leq 3.5$  nsec was obtained for the 3308-keV ( $8^+$ ) level via the 351-keV  $\gamma$  ray. This gives  $B(E2) \geq 44 e^2\text{fm}^4$

for the  $^{92}\text{Zr}$  ( $8^+$ )  $\rightarrow$  ( $6^+$ ) transition which indicates a normal enhancement similar to the situation in  $^{90}\text{Zr}$  where  $B(E2)[8^+ \rightarrow 6^+] = 60.5 \pm 2.5 e^2\text{fm}^4$ ,<sup>1,11</sup> but unlike the situation in  $^{94}\text{Mo}$  where  $B(E2)[8^+ \rightarrow 6^+] \approx 0.11 e^2\text{fm}^4$ .<sup>12</sup>

Another set of  $\gamma$  rays is observed to feed the 1495-keV level, the strongest among them being the 990-keV  $\gamma$  ray. Thus a level is established at 2485 keV. A  $J=3$  or 5 assignment for this level is suggested from the negative  $A_2$  coefficient measured for the 2485-keV  $\rightarrow$  1495-keV  $4^+$  transition, but  $J=5$  is favored by yrast arguments. Previously, a  $5^-$  state had been tentatively assigned to a level at this excitation energy on the basis of ( $p, p'$ ) angular distribution measurements.<sup>13</sup> Also, the 990-keV transition had been observed in an ( $n, n'\gamma$ ) experiment by Fanger *et al.*<sup>5</sup> They suggested an assignment of  $J^\pi = 2^+$  for the 2485-keV level based on an attributed 1103-keV  $\gamma$ -ray branch to the 1383-keV  $0^+$  level. However, their placement of the 1103-keV transition was only based on energy agreement, not on coincidence results; the 1103-keV  $\gamma$  ray was not observed with any strength in the present experiment. Hence, the  $2^+$  assignment for the 2485-keV level, which would also be inconsistent with the present  $\gamma$ -ray angular distribution results, cannot be justified.

In addition to the suggested  $5^-$  level, a  $4^-$  level at  $2740 \pm 10$  keV was recently proposed by Chestnut, Cecil, and McGrath,<sup>6</sup> on the basis of a ( $p, p'$ ) experiment. In the ( $n, n'\gamma$ ) experiment,<sup>5</sup> a level at 2744 keV was observed to undergo  $\gamma$  decay to the 2485-keV ( $5^-$ ), 2339-keV  $3^-$ , and 1495-keV  $4^+$  levels. This decay is consistent with a  $J^\pi = 4^-$  as-

TABLE II. Properties of  $\gamma$  rays assigned to transitions in  $^{92}\text{Zr}$  from the  $^{88}\text{Sr}(^7\text{Li}, p2n)$  reaction.

$E_\gamma$ (keV)	Intensity <sup>a</sup> (relative to 934 keV)	$A_2$	$A_4$	Transition assignment	
				$E_i \rightarrow E_f$ (keV)	$J_i^\pi \rightarrow J_f^\pi$
179.4 $\pm$ 0.5	4	-0.22 $\pm$ 0.12	0.15 $\pm$ 0.14	3998 $\rightarrow$ 3819	(9 <sup>-</sup> ) $\rightarrow$ (8 <sup>-</sup> )
351.3 $\pm$ 0.2	34	0.29 $\pm$ 0.02	-0.08 $\pm$ 0.02	3308 $\rightarrow$ 2957	(8 <sup>+</sup> ) $\rightarrow$ (6 <sup>+</sup> )
439.6 $\pm$ 0.5	7	-0.24 $\pm$ 0.05	-0.04 $\pm$ 0.06	3819 $\rightarrow$ 3379	(8 <sup>-</sup> ) $\rightarrow$ (7 <sup>-</sup> )
561.0 $\pm$ 0.2	83	0.29 $\pm$ 0.01	-0.07 $\pm$ 0.02	1495 $\rightarrow$ 934	$4^+ \rightarrow 2^+$
619 $\pm$ 2	$\sim 7$ <sup>b</sup>			3998 $\rightarrow$ 3379	(9 <sup>-</sup> ) $\rightarrow$ (7 <sup>-</sup> )
650.6 $\pm$ 0.5	9	0.42 $\pm$ 0.09	-0.12 $\pm$ 0.10	4947 $\rightarrow$ 4296	(12 <sup>+</sup> ) $\rightarrow$ (10 <sup>+</sup> )
894 $\pm$ 1	$\sim 18$	0.18 $\pm$ 0.05	-0.03 $\pm$ 0.07	3379 $\rightarrow$ 2485	(7 <sup>-</sup> ) $\rightarrow$ 5 <sup>-</sup>
934.5 $\pm$ 0.2	100	0.27 $\pm$ 0.02	-0.07 $\pm$ 0.02	934 $\rightarrow$ 0	$2^+ \rightarrow 0^+$
987.9 $\pm$ 0.2	19	0.21 $\pm$ 0.08	-0.07 $\pm$ 0.09	4296 $\rightarrow$ 3308	(10 <sup>+</sup> ) $\rightarrow$ (8 <sup>+</sup> )
990.5 $\pm$ 0.2	25	-0.22 $\pm$ 0.06	0.01 $\pm$ 0.08	2485 $\rightarrow$ 1495	$5^- \rightarrow 4^+$
1462.3 $\pm$ 0.5	38	0.20 $\pm$ 0.03 <sup>c</sup>	-0.06 $\pm$ 0.04	2957 $\rightarrow$ 1495	(6 <sup>+</sup> ) $\rightarrow$ 4 <sup>+</sup>

<sup>a</sup> The intensities have about a 10% overall uncertainty.

<sup>b</sup> Estimated from  $\gamma$ - $\gamma$  coincidence.

<sup>c</sup> The  $A_2$  coefficient may be slightly reduced from its full value due to difficulties in separating the Doppler shifted portion of the 1462-keV  $\gamma$  ray at forward angles from background  $\gamma$  rays. The Doppler shift was not included in the peak area analysis.

signment for the 2744-keV level. The results of these previous experiments together with those of the present experiment strongly favor  $J^\pi = 5^-$  for the 2485-keV level.

Several weak  $\gamma$  rays were observed in coincidence with the 990-keV  $5^- \rightarrow 4^-$  transition: 894, 619, 440, and 179 keV. Unfortunately, these  $\gamma$  rays are too weak compared to background  $\gamma$  rays in the singles spectrum to extract their intensities with much confidence. They have been tentatively placed into the  $^{92}\text{Zr}$  level scheme as shown in Fig. 1 based on the  $\gamma$ - $\gamma$  coincidence results and estimated singles and coincidence intensities. The sign of the  $A_2$  coefficient was used together with the assumption of yrast decay to provide tentative  $J$  assignments. A negative parity is inferred for these levels from the fact that the ratio of the partial  $E2$  and  $E1$  widths,  $\Gamma(E2)/\Gamma(E1) = C E_\gamma^5(E2)/E_\gamma^3(E1)$ , where  $E_\gamma$  is in MeV, has typical experimental values of  $C = 1$  to  $100$   $(\text{MeV})^{-2}$  in the mass-90 region compared to the Weisskopf estimate of  $C = 1.4 \times 10^{-5}$   $(\text{MeV})^{-2}$ . Thus, for example, if the 3819-keV level were  $8^+$  rather than  $8^-$ , it would be expected to decay to the 2957-keV ( $6^+$ ) rather than the 3379-keV ( $7^-$ ) level.

#### IV. DISCUSSION

The yrast levels which have been found in  $^{92}\text{Zr}$  (see Fig. 1) can be qualitatively understood with very simple shell-model configurations. The lowest  $0^+$ ,  $2^+$ , and  $4^+$  states are the  $J^\pi$  values expected for the  $(\nu 2d_{5/2})^2$  configuration outside of the  $N = 50$  neutron closed shell. For the positive parity levels, there is then a large gap of about 1.5 MeV to the  $6^+$  and  $8^+$  levels which is related to the energy needed in  $^{90}\text{Zr}$  to excite protons from the semi-closed-shell  $(\pi 2p_{1/2})^2$  configuration to the  $(\pi 1g_{9/2})^2$  configurations. In  $^{90}\text{Zr}$ , the  $6^+$  and  $8^+$  states have excitation energies of 3448 and 3589 keV,<sup>1</sup> respectively. The spacings between the  $8^+$ ,  $10^+$ , and  $12^+$  levels in  $^{92}\text{Zr}$  are very similar to the spacings between the  $0^+$ ,  $2^+$ , and  $4^+$  levels, which suggests a predominantly stretched  $[(\pi g_{9/2})^2 8^+, (\nu d_{5/2})^2 J_n] J = J_n + 8$  configuration for these states. The  $12^+$  state has a unique configuration with  $J_n = 4$ .

The  $^{92}\text{Zr}$   $5^-$  level at 2485 keV can be interpreted as the analog of the  $(\pi g_{9/2} \pi p_{1/2}) 5^-$  configuration in  $^{90}\text{Zr}$  at 2319 keV. Again, the spacings between the tentative  $^{92}\text{Zr}$   $5^-$ ,  $7^-$ , and  $9^-$  levels are very similar to the spacings between the  $0^+$ ,  $2^+$ , and  $4^+$  levels suggesting a predominantly stretched  $[(\pi g_{9/2} \pi p_{1/2}) 5^-, (\nu d_{5/2})^2 J_n] J = J_n + 5$  configuration for the states. The  $9^-$  state has a unique configuration with  $J_n = 4$ .

Shell-model calculations for  $^{92}\text{Zr}$  have been carried out by Vervier<sup>14</sup> assuming the active orbitals  $1g_{9/2}$  and  $2p_{1/2}$  for protons and  $2d_{5/2}$  for neutrons.

More recently, Gloeckner has shown the importance of including the  $3s_{1/2}$  neutron orbital, especially for the more neutron rich Zr isotopes.<sup>15</sup> The experimental levels for  $^{92}\text{Zr}$  are compared with a calculation by Gloeckner<sup>16</sup> in Fig. 4. For this theoretical calculation, the proton-proton interaction matrix elements within the  $g_{9/2}-p_{1/2}$  model space were taken from the seniority conserving interaction which was needed for the  $N = 50$  nuclei.<sup>17</sup> The neutron-neutron interaction matrix elements within the  $d_{5/2}-s_{1/2}$  model space as well as the proton-neutron interaction matrix elements were chosen to give the best overall agreement for energy levels and binding energies of the Zr and Nb isotopes (see column 2 of Tables 1 and 2 in Ref. 16).

The overall comparison between the experimental and theoretical  $^{92}\text{Zr}$  energy levels is good.

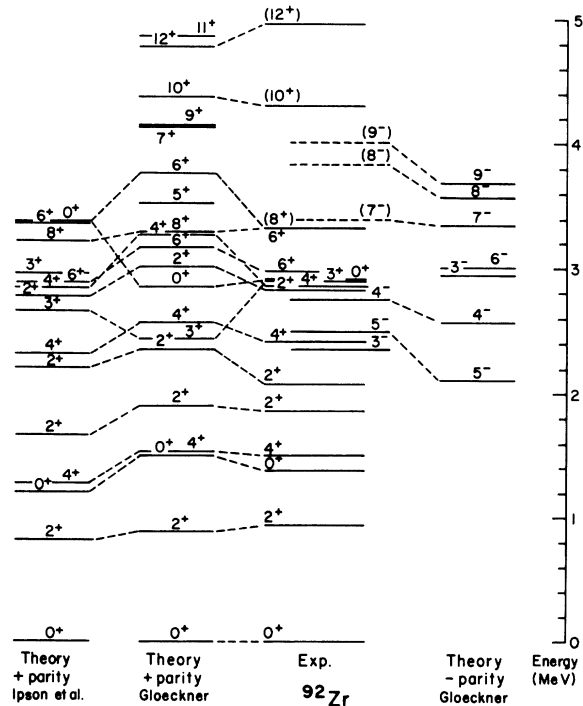


FIG. 4. Comparison of experimental and theoretical energy levels for  $^{92}\text{Zr}$ . The experimental information is from the present work and Refs. 4-7. The theoretical energy levels were calculated by Gloeckner (Ref. 16), assuming  $(\pi p_{1/2})^2 (\nu d_{5/2} \nu s_{1/2})^2$  and  $(\pi g_{9/2})^2 (\nu d_{5/2} \nu s_{1/2})^2$  configurations for the positive-parity levels, and  $(\pi p_{1/2} \pi g_{9/2}) (\nu d_{5/2} \nu s_{1/2})^2$  configurations for the negative-parity levels. Also shown for the positive-parity levels are the theoretical results of Ipson *et al.* (Ref. 7) for which an expanded neutron configuration space of  $(\nu d_{5/2} \nu s_{1/2} \nu d_{3/2} \nu g_{7/2} \nu h_{11/2})^2$  was used. All experimental levels up to 3 MeV and the corresponding theoretical levels are shown, whereas above 3 MeV only the yrast levels are shown.

However, there are some interesting discrepancies. For the positive-parity states, the deviation between theory and experiment is largest for the  $6^+$  and  $12^+$  states; the experimental spacings of the positive-parity states are slightly more even than theoretically predicted. This is indicative of the influence of a vibration-like structure which may be expected in the more neutron rich Zr isotopes.

The 2957-keV  $6^+$  level observed in the present experiment probably corresponds to the 2944-keV level observed in the  $(d, p)$  experiment ( $E_d = 33.3$  MeV) of Bingham and Halbert.<sup>18</sup> They tentatively assign  $l = 4$  ( $1g_{7/2}$ ) to the proton angular distribution for this level, which indicates a  $(\nu 2d_{5/2} \nu 1g_{7/2}) 6^+$  component in addition to the  $[(\pi g_{9/2})^2 J_p, (\nu d_{5/2})^2 J_n] 6^+$  components assumed by Gloeckner. This may explain the relatively poor agreement in this case. Thus, to improve the theoretical agreement for the  $^{92}\text{Zr}$  high-spin positive-parity levels, at least the  $1g_{7/2}$  neutron orbital should be included in the calculation.

Recently, a study of  $^{92}\text{Zr}$  by Ipson *et al.*<sup>7</sup> was published which involved high-resolution  $^{91}\text{Zr}(d, p)$  and  $^{90}\text{Zr}(t, p)$  experiments as well as shell-model calculations that included the  $1g_{7/2}$  and  $1h_{11/2}$  orbitals. The  $(d, p)$  results confirmed the  $l = 4$  assignment for the 2957-keV level, and a  $J^\pi = 6^+$  spin-parity assignment was made on the basis of the  $(d, p)$  and  $(t, p)$  experiments. On the same basis, a  $J^\pi = 6^+$  assignment was made for a state at 3304 keV. The excitation energies and the summed  $1g_{7/2}$  spectroscopic factor that they observed for these two levels are in good agreement with their theoretical calculation. An  $8^+$  level would not have been strongly populated in the  $(d, p)$  or  $(t, p)$  reactions, since the  $(2d_{5/2}, 3s_{1/2}, 2d_{3/2}, 1g_{7/2})^2$  neutron configurations give at most  $J^\pi = 6^+$ , and the  $(1h_{11/2})^2$  configuration is very high in excitation. The  $(8^+)$  assignment to a level at 3308 keV from the present experiment is thus not inconsistent with the results of Ipson *et al.*, assuming that a doublet exists.

The theoretical results of Ipson *et al.* are compared with the calculation of Gloeckner and experiment in Fig. 4. The two  $6^+$  states and the  $8^+ - 6^+$  energy spacing are better described by the more complete calculation of Ipson *et al.*; however, the fact that some states, including the lowest  $4^+$  state, are not in as good agreement as in Gloeckner's calculation indicates that some adjustment of the two-body matrix elements is needed.

The theoretical results for the negative-parity states within the more complete model space were not given in Ref. 7.

All of the negative-parity levels except the  $7^-$  level are predicted to be 200–300 keV too low in Gloeckner's theoretical calculation. This disagreement is very similar to the situation in  $^{91}\text{Zr}$  for the  $\frac{15}{2}^-$  level,<sup>10, 16</sup> and in  $^{94}\text{Zr}$  and  $^{96}\text{Zr}$  for the  $5^-$  levels.<sup>16</sup> The disagreement cannot be entirely due to perturbations from the  $(\nu 2d_{5/2})^n \nu 1h_{11/2}$  configurations, since the  $^{91}\text{Zr}$  ( $n = 0$ )  $\frac{15}{2}^-$  and  $^{92}\text{Zr}$  ( $n = 1$ )  $9^-$  levels cannot be formed in this way. Part of the disagreement for the negative-parity levels may be related to the fact that the  $^{90}\text{Zr}$   $5^-$  state may have a more complex structure, involving the  $2p_{3/2}$  and  $1f_{5/2}$  proton-hole orbitals, than the simple  $1g_{9/2} 2p_{1/2}$  configuration assumed in the theoretical calculation.

In summary, the overall agreement of Gloeckner's shell-model calculation for  $^{92}\text{Zr}$  with the experimental levels is good, but if the agreement is to be improved further, many more model-space orbitals involving both neutron particles and proton holes must be considered. Such large shell-model calculations involving, in this case, up to nine active orbitals are difficult to carry out exactly. However, a simplification is suggested by the fact that many features of the  $N = 51$  and  $52$  spectra can be understood in terms of a weak coupling between the proton and neutron degrees of freedom. This may be partially justified because the proton-neutron interaction is weaker than the interaction between like particles. Although many single-particle orbitals may be important in the exact calculations for the pure neutron and proton systems independently, the weak coupling idea suggests, for example, that the combined neutron-proton multiparticle systems depend mainly on the lowest few eigenstates of a given spin of the pure neutron and proton systems, and that a truncation involving the higher eigenstates of a given spin in the pure systems can be used. This truncation scheme was used by Ipson *et al.*<sup>7</sup> for the positive-parity levels. It would be interesting to carry out similar calculations for the negative-parity levels.

Experimentally, more information is needed to confirm the high-spin negative-parity states suggested by the present experiment. In particular, it would be interesting to carry out a high resolution  $(p, p')$  experiment similar to the  $^{91}\text{Zr}$  study of Blok,<sup>19</sup> which was sensitive to configurations involving the  $^{90}\text{Zr}$   $3^-$  and  $5^-$  levels.

† Work supported in part by the National Science Foundation.

\* Present address: Physics Department, Michigan

State University, East Lansing, Michigan.

‡ Present address: Brooklyn College, City University of New York, Brooklyn, New York.

- <sup>8</sup>Present address: University of Auckland, New Zealand.
- <sup>1</sup>D. C. Kocher, Nucl. Data Sheets 16, 55 (1975).
- <sup>2</sup>J. O. Newton, in *Nuclear Spectroscopy and Reactions*, edited by J. Cerny (Academic, New York, 1974), part C, pp. 185–227; J. R. Grover, Phys. Rev. 157, 832 (1967).
- <sup>3</sup>P. M. S. Lesser, B. A. Brown, D. B. Fossan, and A. R. Poletti, Bull. Am. Phys. Soc. 19, 473 (1974).
- <sup>4</sup>D. C. Kocher and D. J. Horen, Nucl. Data Sheets B7, 229 (1972).
- <sup>5</sup>U. Fanger, D. Heck, R. Pepelnik, H. Schmidt, and J. Wood, in *Contributions to the Conference on Nuclear Structure Study with Neutrons, Budapest, Hungary, 1972*, edited by J. Erö and J. Szücs (Central Research Institute for Physics, Budapest, 1974), p. 72.
- <sup>6</sup>R. P. Chestnut, F. E. Cecil, and R. L. McGrath, Phys. Rev. C 10, 2434 (1974).
- <sup>7</sup>S. S. Ipson, K. C. McLean, W. Booth, J. G. B. Haigh, and R. N. Glover, Nucl. Phys. A253, 189 (1975).
- <sup>8</sup>B. A. Brown, P. M. S. Lesser, and D. B. Fossan, Phys. Rev. Lett. 34, 161 (1975).
- <sup>9</sup>B. A. Brown, D. B. Fossan, and P. M. S. Lesser, Phys. Rev. C 13, 1900 (1976).
- <sup>10</sup>B. A. Brown, D. B. Fossan, and P. M. S. Lesser (unpublished).
- <sup>11</sup>K. G. Lobner, Nucl. Phys. 58, 49 (1964).
- <sup>12</sup>C. M. Lederer, J. M. Jaklevic, and J. M. Hollander, Nucl. Phys. A169, 449 (1971).
- <sup>13</sup>J. K. Dickens, E. Eichler, and G. R. Satchler, Phys. Rev. 168, 1355 (1968).
- <sup>14</sup>J. Vervier, Nucl. Phys. 75, 17 (1966).
- <sup>15</sup>D. Gloeckner, Phys. Lett. 42B, 381 (1972).
- <sup>16</sup>D. Gloeckner, Nucl. Phys. A253, 301 (1975).
- <sup>17</sup>D. Gloeckner, and F. J. D. Serduke, Nucl. Phys. A220, 477 (1974).
- <sup>18</sup>C. R. Bingham and M. L. Halbert, Phys. Rev. C 2, 2297 (1970).
- <sup>19</sup>H. P. Blok, Ph.D. thesis, Vrije Universiteit, Amsterdam, 1972 (unpublished); H. P. Blok, L. Hulstman, E. J. Kaptein, and J. Block (unpublished).